Photosynthetic Model Membranes of Natural Plant Thylakoid Embedded in a Patterned Polymeric Lipid Bilayer

Yoneda, Takuro
Tanimoto, Yasushi
Takagi, Daisuke
Morigaki, Kenichi

(Citation)
Langmuir,36(21):5863-5871

(Issue Date)
2020-05-09

(Resource Type)
journal article

(Version)
Accepted Manuscript

Photosynthetic model membranes of natural plant thylakoid embedded in a patterned polymeric lipid bilayer.

Takuro Yoneda [1], Yasushi Tanimoto [1], Daisuke Takagi [1, 2], Kenichi Morigaki [1, 3] *

1: Graduate School of Agricultural Science, Kobe University, Rokkodaicho 1-1, Nada, Kobe 657-8501 Japan

2: Graduate School of Agricultural Science, Tohoku University, Aoba 468-1, Aranaki, Aoba, Sendai 980-0845 Japan

3: Biosignal Research Center, Kobe University, Rokkodaicho 1-1, Nada, Kobe 657-8501 Japan

*Corresponding author:

Kenichi Morigaki: E-mail: morigaki@port.kobe-u.ac.jp, Fax: +81-78-803-5941

Abstract

Thylakoid membranes in the chloroplast of plants, algae, and cyanobacteria are the powerhouse of the photosynthesis capturing solar energy and converting it into chemical energy. Although their structure and function have been extensively studied, the intrinsically heterogeneous and dynamic nature of the membrane structures are still not fully understood. Investigating native thylakoid membranes *in vivo* is difficult due to their small size and limited external access to the chloroplast interior, while the bottom-up approaches based on model systems have been hampered by the sheer complexity of the native membrane. Here we try to fill the gap by reconstituting the whole thylakoid membrane into a patterned substrate-supported planer bilayer. A mixture of thylakoid membrane purified from spinach leaves and synthetic phospholipid (DOPC) vesicles spontaneously formed a laterally continuous and fluid two-dimensional (2D) membrane in the scaffold of patterned polymeric bilayer. Chlorophyll fluorescence arising from photosystem II (PSII) recovered after photobleaching, suggesting that the membrane components are laterally mobile. The reversible changes of chlorophyll fluorescence in the presence of the electron acceptors and/ or inhibitors indicated that the electron transfer activity of PSII was retained. Furthermore, we confirmed the electron transfer activity of photosystem I (PSI) by observing the generation of NADPH in the presence of water-soluble ferredoxin and ferredoxin-$NADP^+$ reductase. The lateral mobility of membrane-bound molecules and the functional reconstitution of major photosystems provide evidence that our hybrid thylakoid membranes could be an excellent experimental platform to study the 2D molecular organization and machinery of photosynthesis.

Introduction

In plants, algae, and cyanobacteria, the photosynthetic electron transfer reactions take place in the thylakoid membrane[1-3]. The membrane structure is essential for the photosynthetic energy conversion. Conceptually, the process starts with the capture of solar energy by chlorophyll in light-harvesting complex (LHC) proteins that transfer energy as excited electronic states to two photosystem protein complexes (PSII and PSI). PSII performs a light-induced water-splitting reaction to supply electrons to PSI via electron mediators, whereas PSI provides electrons for generating the energy-rich coenzyme NADPH. The structure of thylakoid membrane dictates the electron flow by the distribution, lateral diffusion, and complex formation of the membrane-bound proteins. A proton gradient is generated across the membrane in conjunction with the electron transfer via photooxidation of water in PSII and oxidation of reduced plastoquinone (PQ) by cytochrome *b*$_6$*f* (cyt *b*$_6$*f*) complex. The proton gradient is further used for generating ATP by the ATP synthase protein complex, and it also acts as a trigger to induce a heat dissipation system that converts excess light energy into heat[4,5]. It is known that LHCII diffuse in the membrane to balance the excitation energy between PSII and PSI under fluctuating light conditions[6,7]. However, how the two dimensional organization of thylakoid membrane including membrane proteins and lipids regulates the photosynthetic functions is not fully understood due to the lack of methodologies to study the molecular details of membrane organization and functions in a natural state.

The structural organization of thylakoid membranes have been extensively studied by biochemical, spectroscopic, and microscopic techniques. Cryo-electron tomography (cryo-ET) has allowed the visualization of thylakoid membrane within native-like

chloroplasts. By using serial sections of stained chloroplasts that are cryo-immobilized and dehydrated, the 3D thylakoid membrane structure, stacked region (grana) and non-stacked region (stroma lamella), could be revealed[8,9]. Although electron microscopy provides important knowledge about internal structure of chloroplast, observation of molecular dynamics in the thylakoid membrane is not possible because samples need to be immobilized and sectioned. Recently, atomic force microscopy (AFM) observations of thylakoid membranes adsorbed on solid supports are revealing details of the molecular organization within the membrane[10-12]. Furthermore, purified components of photosynthetic machinery (LH2 and LH1-reaction center complex isolated from purple bacteria, or solo-LHCII isolated from land plants, etc.) have been reconstituted in a substrate-supported model membranes to study their lateral organization[13-15], clustering[16,17], membrane stacking[18-20] and potential as nanomaterials[21]. Supported membrane systems are amenable to highly sensitive interfacial analyses (including AFM) and they can be generated in a designed pattern[22-25], which greatly enhances their utility in analyzing the photosynthetic reactions. However, the studies using supported membranes thus far had only two choices, *i.e.*, adsorbed thylakoid membranes or single components reconstituted in a lipid membrane. Generation of a hybrid system from native thylakoid membrane and purified lipids/ protein components as a continuous and laterally mobile lipid membrane could vastly expand the flexibility of experimental designs to investigate the photosynthetic machinery. These hybrids could provide the benefits of amenability to sensitive analyses and act as a model which better represents the complexity of the natural system than simpler lipid bilayers.

Here, we describe a methodology to integrate the thylakoid membrane into a patterned,

continuous 2D membrane on a glass substrate (Figure 1). Previously, we developed a methodology for fabricating patterned lipid membranes based on the lithographic photo-polymerization of lipid bilayer[26,27]. These studies showed that biologically relevant lipid membranes can be incorporated into the patterned scaffold of polymeric bilayer. Confining the biologically relevant membranes in well-defined geometries can facilitate their quantitative evaluation by highlighting the region of interest. Furthermore, the bilayer edges of polymeric bilayer can enhance the formation of fluid lipid bilayers by catalyzing the rupture of vesicles[28]. In the current study, this strategy has been extended for application to photosynthesis, by introducing thylakoid membranes into the corrals between preformed polymeric bilayers. The hybrid thylakoid membrane retained the lateral mobility of molecules (fluidity) and the activity of PSI and PSII. By preparing a 2D planar thylakoid membrane, we can evaluate the photosynthetic functions with high sensitivity and spatial resolution.

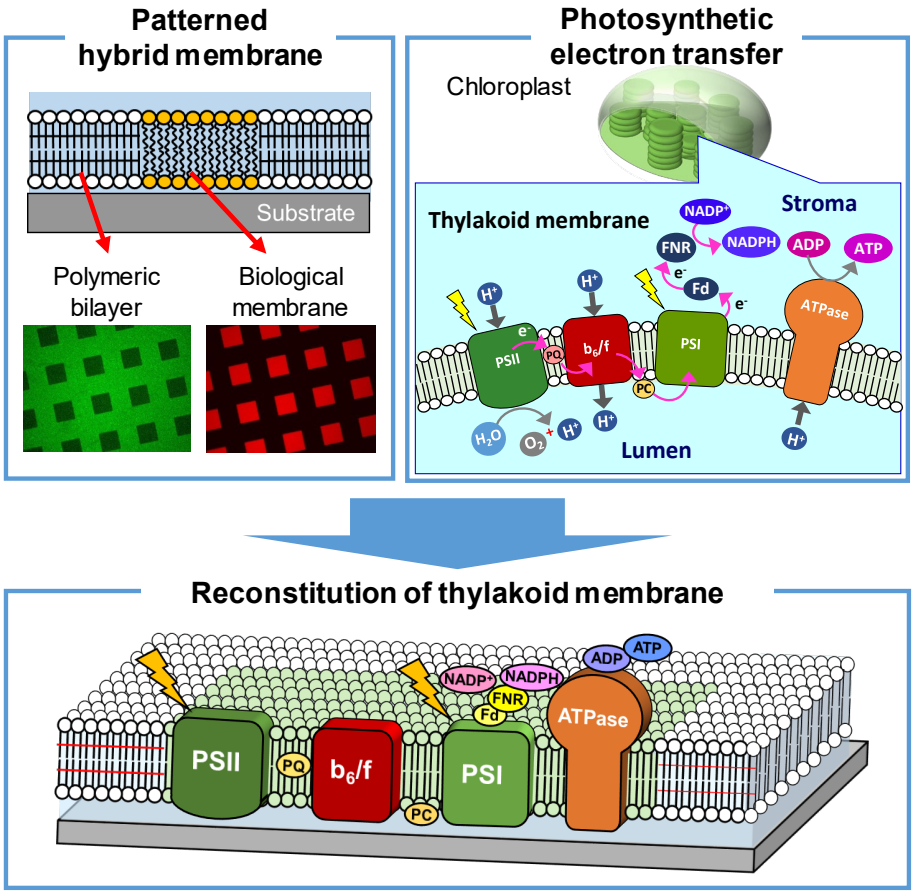

Figure 1. Schematic outline of thylakoid membrane as a patterned, continuous two-dimensional membrane on a glass substrate.

Materials and Methods

Materials

1,2-bis(10,12-tricosadiynoyl)-*sn*-glycero-3-phosphocholine (DiynePC) and 1,2-dihexanoyl-*sn*-glycero-3-phosphocholine (DHPC-C6) were purchased from Avanti Polar Lipids (Alabaster, AL). 1,2-dioleoyl-*sn*-glycero-3-phosphocholine (DOPC) was purchased from NOF (Tokyo, Japan). *N*-(7-nitrobenz-2-oxa-1,3-diazol-4-yl)-1,2-dihexadecanoyl-*sn*-glycero-3-phosphoethanolamine, triethylammonium salt (NBD-PE) was purchased from Molecular Probes (Eugene, OR). 2,6-dimethybenzoquinone (DMBQ), 3-(3,4-dichlorophenyl)-1,1-dimethylurea (DCMU), 2,6-dichloroindophenol (DCIP), hydroxylamine, nigericin sodium salt, ferredoxin (Fd) from *Spinacia oleracea* (spinach), and ferredoxin-$NADP^+$ reductase (FNR) from *Spinacia oleracea* (spinach) were purchased from Sigma-Aldrich (St. Louis, MO). L(+)-ascorbic acid, sodium dodecyl sulfate (SDS) and β-nicotinamide adenine dinucleotide phosphate sodium salt ($NADP^+$) were purchased from Nacalai Tesque (Kyoto, Japan). The deionized water used for cleaning the substrates and preparing all aqueous solutions for samples was ultrapure Milli-Q water (Millipore) with a resistance of 18.2 MΩ cm.

Isolation of thylakoid membranes from spinach

Thylakoid membranes were purified from spinach (*Spinacia oleracea*) leaves obtained from a local market by the well-established percoll density gradient centrifugation method according to the previous report (Supporting Information)[29]. The isolated thylakoid membranes were fragmented by passing through high-pressure homogenizer (Parr Instrument Company, Moline, IL) twice. The chlorophyll concentration was determined by the method of Arnon[30]. The thylakoid membranes were stored in stock

buffer (50 mM KH_2PO_4 (pH 7.5), 10 mM NaCl, 2 mM $MgCl_2$ and 330 mM sorbitol) at -80°C.

Substrate cleaning

Microscopy coverslips (Matsunami, Osaka, Japan) made of borosilicate glass were used as the substrates for bilayer deposition. The substrates were sonicated in an SDS solution (0.1 M) for 20 min, rinsed with Milli-Q water (Millipore), treated in a solution of NH_4OH (28%)/H_2O_2 (30%)/H_2O (0.05:1:5) for 10 min at 65°C, rinsed extensively with Milli-Q water, and stored in Milli-Q water. Before use, the substrates were dried with nitrogen gas and further cleaned by the UV/ozone treatment for 20 min (PL16-110; Sen Lights, Toyonaka, Japan).

Preparation of patterned polymeric bilayer

Bilayers of monomeric DiynePC were deposited onto glass substrates by the spontaneous spreading of vesicles, as outlined below. DiynePC powder was suspended in Milli-Q water and DHPC-C6 was added to the solution to accelerate the fusion of vesicles (the final concentrations of DiynePC and DHPC-C6 were 3 mM and 0.14 mM, respecively)[31]. The mixture was frozen in liquid nitrogen and thawed at 60°C (five cycles). After the freeze-and-thaw, DiynePC suspensions were homogenized by an ultrasonic homogenizer (Branson Sonifier 150, Branson Ultrasonics, Danbury, CT) at 60°C and the power setting of 3 W (30 s × 2). Monomeric DiynePC suspensions were deposited onto a cleaned substrate on ice to immediately cool the membrane. (we previously discovered it is important to deposit monomers at a low temperature in order to generate homogeneous polymeric DiynePC bilayers[32]).

Polymerization of DiynePC bilayers was conducted by UV irradiation using a mercury lamp (SP9; Ushio, Tokyo, Japan) as the light source. A closed system that comprised a water reservoir, a pump, and a chamber (～4 mL volume) was used. The water reservoir was depleted of oxygen by purging with argon, and oxygen-free water was continuously supplied to the chamber by the pump. The chamber had two walls on the opposite sides, one being the sample (the lipid bilayer was inside the chamber) and the other being a quartz window through which UV light was illuminated. The desired patterns were transferred to the lipid bilayer in the polymerization process by illuminating the sample through a photomask (photomask was placed directly on top of the monomeric bilayer). After sufficient circulation of deaerated water (typically 15 min), the pump was stopped and the polymerization was started. The applied UV intensity was typically 16 mW/cm^2 at 254 nm (UIT-250 Ushio, Tokyo, Japan). After the UV irradiation, nonpolymerized DiynePC molecules were removed from the substrate surface by immersing in 0.1 M SDS solution at 30°C for 30 min and rinsing with Milli-Q water extensively. The polymerized bilayers were stored in Milli-Q water in the dark at 4°C.

Preparation of vesicle suspensions

Lipids dissolved in chloroform (DOPC with 1mol% NBD-PE) were mixed in a round-bottom flask, dried under a stream of nitrogen, and subsequently evaporated for at least 4 h in a vacuum desiccator. The dried lipid film was hydrated in the stock buffer (50 mM KH_2PO_4 (pH 7.5), 10 mM NaCl, 2 mM $MgCl_2$ and 330 mM sorbitol) to a final lipid concentration of 1 mM. Lipid membranes were dispersed by five freeze/thaw cycles for effectively detaching the lipid layers from the glass surface. The suspension was sonicated

on ice by the ultrasonic homogenizer with the power of 3 W (30 s × 4) before use to generate DOPC small unilamellar vesicles. The average sizes of vesicle suspensions were evaluated by the dynamic light scattering (ELSZ-1000, Otsuka Electronics, Tokyo, Japan).

Incorporation of thylakoid membrane into the patterned polymeric bilayer

The substrate with a patterned polymeric bilayer was dried with nitrogen, and a cell was made by attaching an elastic sheet of poly(dimethylsiloxane) (PDMS, Silpot184, Toray Dow Corning, Tokyo, Japan) having a circular hole (12 mm). Thylakoid membranes fragmented by the high-pressure homogenizer were mixed with sonicated DOPC vesicles in the lipid ratio of 1:1 (w/w), unless otherwise stated. 0.5 mM DOPC is 0.393 mg lipid/mL (MW=786.13). From the previous literature, we assumed 1 mg chl/mL corresponded to 3.254 mg lipid/mL[33]. Based on this relation, 0.121 mg chl/mL were calculated to be equivalent to 0.5 mM of DOPC.

100 μL of the mixed solution was introduced into the PDMS cell and incubated for 30 min. Thus formed membrane was then rinsed 10 times with stock buffer. The prepared whole thylakoid membrane contained both appressed (grana) and non-appressed (stroma lamellae) thylakoid membranes.

Fluorescence microscopy observation

Fluorescence microscopy observation was performed using an inverted microscope (IX-73, Olympus, Tokyo, Japan) equipped with a xenon lamp (UXL-75XB, Olympus), 20x objective (NA 0.75) or 100x objective (NA 1.49), and a CMOS camera (Orca 4.0, Hamamatsu Photonics, Hamamatsu, Japan). Two types of filter sets were used: (1) excitation 470−490 nm/ emission 510−550 nm for observing fluorescence of NBD-PE

and DiynePC (green fluorescence). (2) Excitation 630–650 nm/ emission 671–693 nm for observing chlorophyll fluorescence of PSII (red fluorescence).

Quartz crystal microbalance with dissipation (QCM-D) measurement

QCM-D measurements were performed by using a Q-Sense E1 system with a flow module (Biolin Scientific, Gothenburg, Sweden). Quartz crystals with a thin SiO_2 layer were used as the sensors. The sensor crystals were cleaned in 0.1 M SDS solution (immersed for 30 min at 30°C), rinsed with deionized water, dried under a nitrogen stream. For the measurements, the sensor crystal was oscillated at its resonance frequency of 5 MHz and at three harmonics (25, 35, 45 MHz), and the shifts of frequency (Δf) and dissipation (ΔD) were monitored. The interval for data acquisition was 0.2 s. The mounted QCM sensor crystal was first equilibrated with a degassed buffer solution at 21.8°C. The buffer solution was subsequently replaced with the vesicle/ thylakoid membrane suspensions.

Measurement of NADPH fluorescence (PSI activity)

To confirm the activity of PSI in the hybrid thylakoid membrane, we monitored generation of NADPH. The activity of PSII was inhibited by adding 20 μM DCMU. 150 μM DCIP reduced by 10 mM ascorbic acid was added as the electron donor to PSI. 1 μM Fd, 500 nM FNR, and 200 μM $NADP^+$ were added to the aqueous solution. In order to prevent the electron transfer activity from being rate-controlled by the formation of membrane potential, nigericin was added as an uncoupler. After irradiating with white light (100 μmol photons m^{-2} s^{-1}), the aqueous solution (300 μL) was collected from the PDMS cell. Fluorescence of NADPH in the collected solution was measured (excitation:

340 nm; emission: 400-600 nm) (F-2500, Hitachi, Japan). For obtaining the time course of PSI assay, we repeated the measurements by returning the aqueous solution to the reaction chamber and further illuminating the thylakoid membrane. The activity of the whole electron transfer chain from PSII to PSI was assayed using the same method except that DCMU, DCIP and ascorbic acid were not added.

Results and discussion

We formed the patterned polymeric framework as an array of 20x20 μm square-shaped empty regions termed "corrals", as described in our previous publications (as detailed in the methods section)[32,34]. These bilayers made of polymerized lipid molecules were then used as a template for assembly of thylakoid membranes extracted from spinach chloroplasts. If we applied a suspension of isolated thylakoid membrane on their own, membrane fragments were found randomly adsorbed on the polymeric bilayers and in the corrals, as was indicated in epifluorescence microscopy images by the red fluorescence from chlorophyll within PSII and LHCII as compared to the green fluorescence from the polymerized bilayer framework (Figure 2A-C). The membranes did not spontaneously fuse with each other and remained isolated from each other. To promote the formation of a continuous planar bilayer from thylakoid membrane, we mixed thylakoid membrane with sonicated DOPC vesicles. Previous studies have shown that co-application of phospholipid vesicles facilitated the transformation of vesicular biological membranes into a planar membrane on the substrate by the fusogenic effects of ruptured phospholipid vesicles patches[35,36]. Figure 2D-F show fluorescence microscopy observation of the hybrid thylakoid membrane (red fluorescence) and polymeric bilayer (green fluorescence) formed from incubating substrates with a 1:1 mixture of extracted thylakoid: DOPC vesicles (w/w of the lipids). The lipid content in thylakoid membrane was estimated from the chlorophyll concentration (0.121 mg /mL)[33], and the concentration of DOPC was 0.5 mM. The sizes of thylakoid membrane and DOPC vesicles were reduced by the high-pressure homogenizer and sonication, respectively, since it is well documented that smaller vesicles are more effective in forming a planar membrane[37]. The mean diameter of sonicated DOPC vesicles determined by the dynamic

light scattering was 124 nm, whereas that of thylakoid could not be determined due to the size heterogeneity. Figure 2D shows a homogeneous distribution of chlorophyll fluorescence in the corrals. This suggests that the thylakoid membranes have spread relatively evenly at the micrometer scale. When the lipophilic fluorophore NBD-PE is incorporated into DOPC vesicles, the fluorescence from NBD-PE was also observed in the same corrals as chlorophyll, suggesting that both thylakoid membrane and DOPC bilayer were homogeneously mixed (Figure 3). It is at present not well characterized if DOPC vesicles and thylakoid membranes fuse with each other in the suspended state, diluting the proteins in thylakoid membranes and making spreading on the substrate surface easier, or two types of membranes independently adsorb and rupture on the surface. Preceding studies have shown that thylakoid membranes can fuse with lipid vesicles and spread on the lipid membrane surface as a planar patch of membrane[38,39].

The continuity and fluidity of incorporated thylakoid membrane was evaluated by fluorescence recovery after photobleaching (FRAP) (Figure 3). After locally photobleaching either chlorophyll or NBD-PE lipid molecules in the corrals, the boundaries between the bleached and non-bleached regions became blurred over time. Apparently, continuous and fluid lipid bilayers were formed with the mobility of the lipids and the chlorophyll-containing proteins (PSII and LHCII). Formation of a planar membrane on the polymeric patterned substrates was further accessed by the QCM-D measurements. Figure 4 shows the frequency shift and dissipation profiles. As we applied DOPC vesicles alone, we observed that both frequency and dissipation shifts (Δf, ΔD) went through an inflection point, as is characteristic for the transformation of spherical vesicles into planar bilayers[40]. The Δf stabilized at approx. -30 Hz typical for a high

quality lipid bilayer. If only thylakoid suspensions were introduced to the silica-covered sensor surface, we observed monotonic shifts of the frequency and dissipation, suggesting adsorption of vesicular particles onto the surface. Introduction of mixtures of thylakoid membrane and DOPC significantly altered the QCM-D profiles. The frequency shift showed an inflection point, indicating that a planar membrane was formed from a mixture of thylakoid and DOPC membranes (Figure 4). The dissipation shift remained monotonic but larger compared with thylakoid only, suggesting the accumulation of soft membrane layers. The observation that the final Δf, ΔD for hybrid thylakoid/DOPC membranes was significantly larger than for DOPC alone may suggest that loosely associated vertically protruded objects were associating with the planar membrane and/or that the overall area density is higher (the greater Δf suggests a greater overall mass added and the greater ΔD suggests a more flexible layer).

In order to study the role of DOPC vesicles in promoting the fusion of thylakoids, we changed the ratio of thylakoid membrane and DOPC/ NBD-PE and observed the membrane formation in the corrals (Figure 5). The concentration of DOPC was fixed (0.5 mM) and that of thylakoid membranes was changed to give suspensions with a range of mixing ratios 0.25/1, 0.5/1, 0.75/1, 1/1, 1.5/1, 1.75/1, 2/1, 3/1 (w/w of the lipids). This equates to a fraction of lipids from thylakoid with respect to the total lipid 0.20, 0.33, 0.43, 0.5, 0.6, 0.64, 0.67, and 0.75, respectively. The thylakoid membrane could be reconstituted into the patterned polymeric bilayers for all conditions (Figure 5A). The area fraction of reconstituted thylakoid membrane was estimated from the fluorescence intensity of NBD-PE in the corral, assuming that it represents the membrane area fraction that originates from DOPC. In other words, we assume the thylakoid membrane replaces

the DOPC and NBD-PE and thus reduces the relative fluorescence from NBD-PE. From the fluorescence intensities of NBD-PE in pure DOPC bilayer (I_{DOPC}) and in the mixed bilayer (I_{mix}), the area fraction of thylakoid membrane as estimated from the relative lipid fraction was calculated using the following equation.

$$F_{thy} = 1 - I_{mix}/I_{DOPC}$$

The area fraction increased linearly with the concentration of thylakoid membrane in the starting mixture in suspension (Figure 5B). Furthermore, the chlorophyll fluorescence also linearly increased with the area fraction of thylakoid membrane (Figure 5C), as expected if the thylakoids contain a consistent amount of chlorophyll-containing proteins after their incorporation. These results demonstrate our ability to tune the density of thylakoid-derived membrane in the hybrid bilayer system. It would therefore be possible to examine the effect of molecular crowding on the lateral diffusion of membrane components[39].

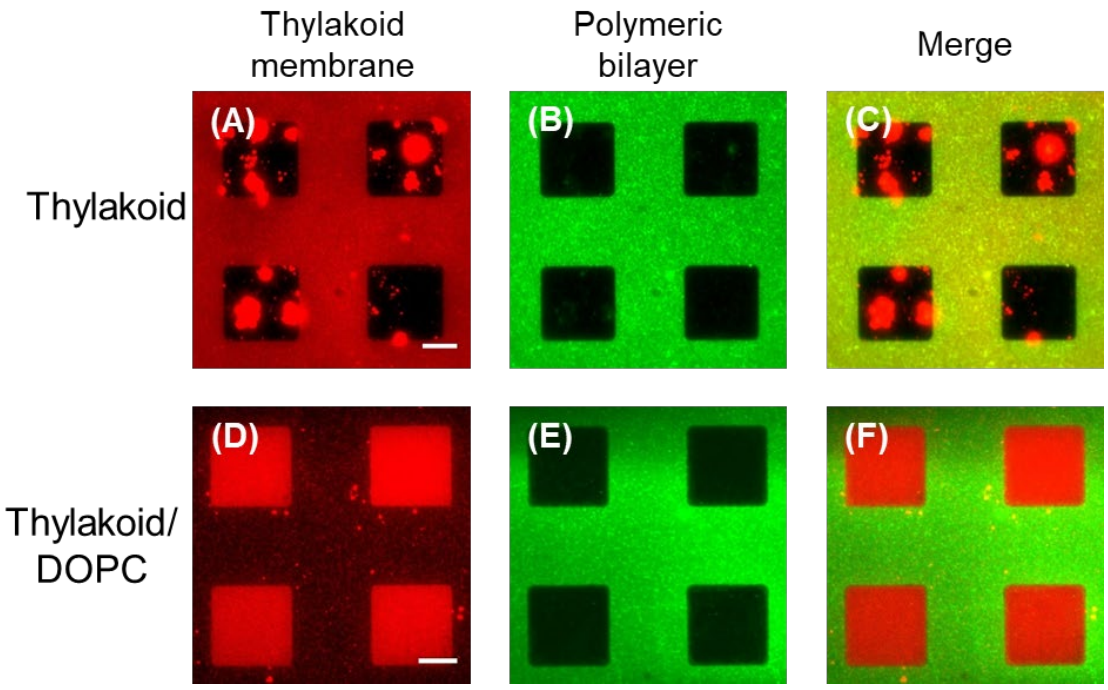

Figure 2. Epifluorescence microscopy images showing the generation of hybrid model membranes by incorporation of thylakoid membranes into the scaffold of patterned polymeric bilayers. (A-C) Introduction of thylakoid membrane alone (without DOPC vesicles). (D-F) Thylakoid membranes introduced with DOPC vesicles. (A, D) Red fluorescence from chlorophyll of PSII and LHCII in the thylakoid membrane. (B, E) Green fluorescence from polymeric bilayers. (C, F) Merged images of thylakoid membranes and polymeric bilayers. Note, there is negligible fluorescence in the red channel before the addition of thylakoid or DOPC. No NBD-PE was used here. The brightness and contrast of the micrographs were adjusted for clarity. The scale bar corresponds to 10 μm.

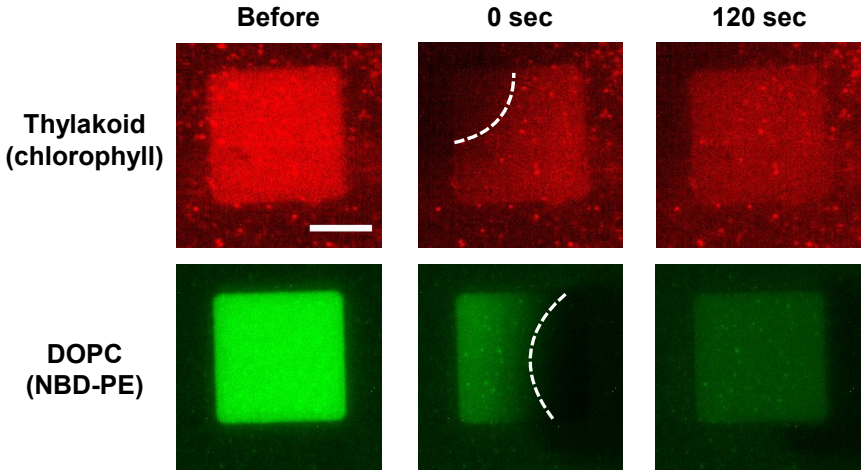

Figure 3. Fluorescence microscopy with FRAP of the incorporated thylakoid/ DOPC membrane. This hybrid membrane sample was formed from thylakoid membranes mixed with DOPC vesicles containing 1mol% NBD-PE, which represents the spatial location of lipids. Fluorescence of chlorophyll from thylakoid membrane (upper panels) and NBD-PE from DOPC (lower panels) was locally photobleached in a corral and recovery of fluorescence due to lateral diffusion of the fluorophore was monitored. The images were captured before, just after (0 sec), and 120 sec after the photobleaching. The dashed lines indicate the boundary of the photobleached regions. The scale bar corresponds to 10 μm.

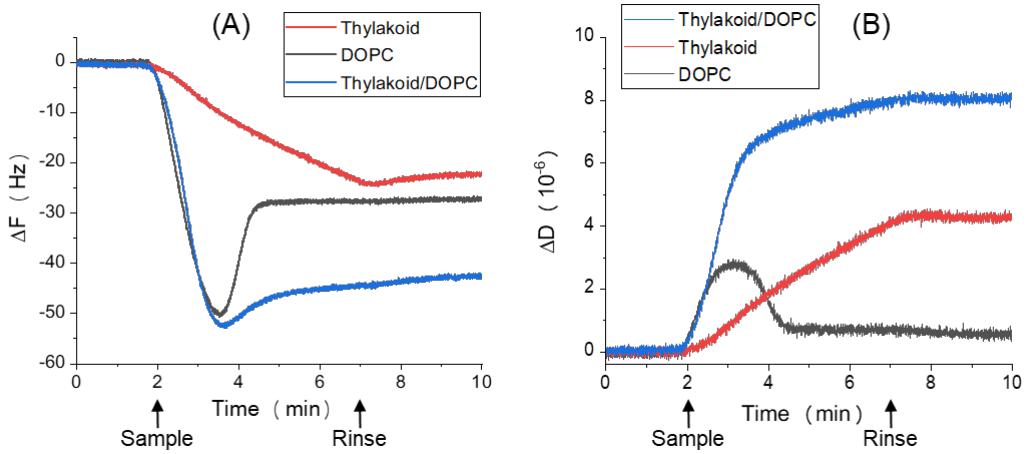

Figure 4. QCM-D profiles for the adsorption of thylakoid and DOPC vesicles. The shifts of frequency (Δf) and dissipation (ΔD) were plotted versus incubation time for thylakoid (red), DOPC (black), and thylakoid/ DOPC mixture (blue).

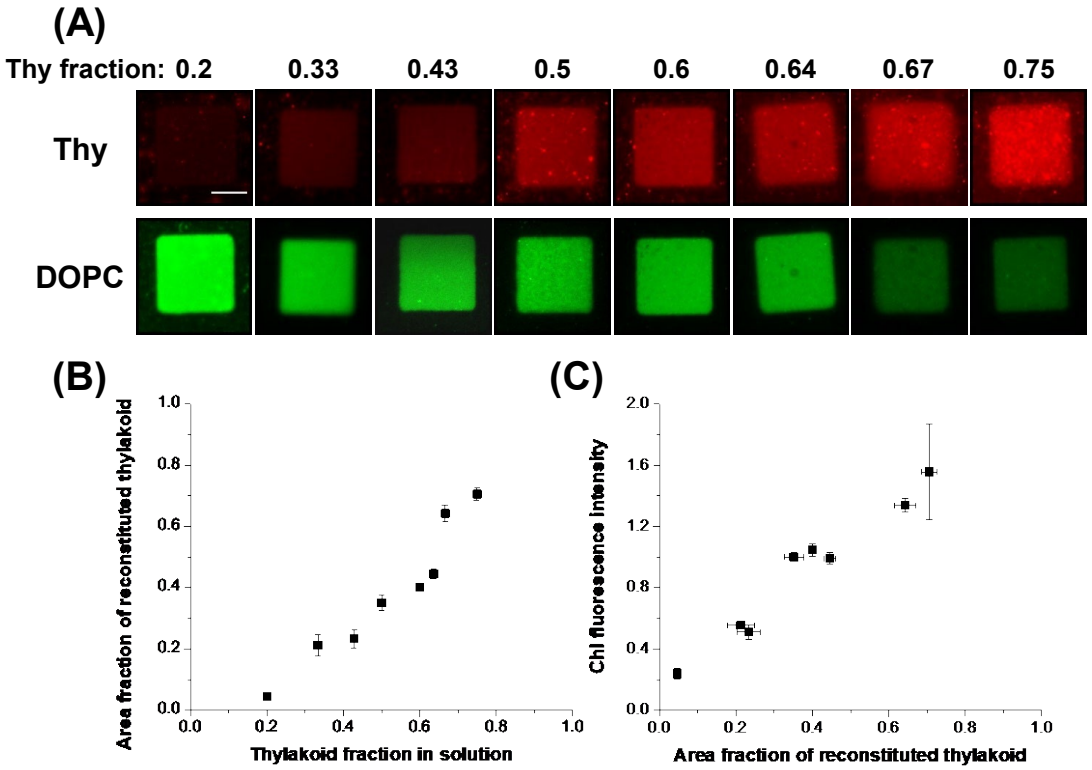

Figure 5. Fluorescence microscopy and graphical analysis of the generation of hybrid thylakoid/ DOPC membranes with varied lipid ratios. DOPC vesicles contained 1mol% NBD-PE for all samples. (A) Chlorophyll fluorescence from thylakoid membrane (red) and NBD-PE fluorescence from DOPC (green). The numbers at the top are the fractions of thylakoid lipids in thylakoid/ DOPC mixtures in solutions (estimated as weight/ weight). The scale bar corresponds to 10 μm. (B) The area fraction of thylakoid membranes incorporated in the corrals was estimated from the fluorescence intensity of NBD-PE. (C) Chlorophyll fluorescence intensity was plotted versus the area fraction of incorporated thylakoid. The fluorescence intensities were normalized to the chlorophyll fluorescence intensity of the standard mixing ratio of 1:1. N= 3 substrates. Error bars represent the standard deviation.

The electron transfer activity of PSII in the hybrid thylakoid membrane was evaluated by observing the chlorophyll fluorescence emission from LHCII and PSII reaction center (Figure 6). The logic of this well-established assay[29,41] is that energy from photo-excited electronic states of chlorophyll within these proteins is dissipated as fluorescence if the primary quinone electron acceptor (Q_A)-reduction within PSII is suppressed by hindering the latter photosynthetic electron transfer reactions relaying to PSI and further reaction systems. In the absence of the water-soluble proteins ferredoxin (Fd) and ferredoxin-$NADP^+$ reductase (FNR), which naturally associate with PSI, the absorbed light energy is expected to be primarily released as chlorophyll fluorescence due to the blockage of electron transfer (refer to schematic in Figure 1). Thus, our hybrid membranes without further intervention show a relatively high chlorophyll fluorescence (Figure 6A). Chlorophyll fluorescence decreased as an electron acceptor, DMBQ (500 μM), was added due to the electron transfer from PSII-LHCII (Figure 6B, D). The assumption that the chlorophyll fluorescence in panel (A) arose from the hindered electron transfer was further supported by adding hydroxylamine, which is known to dissociate PSII manganese (Mn) clusters and block the photosynthetic electron transfer reaction to regenerate the reaction center chlorophyll (P680) within PSII. As we added hydroxylamine (100 mM) to the thylakoid membranes in the presence of DMBQ, the chlorophyll fluorescence recovered (Figure 6C, D). Although hydroxylamine can potentially act as an electron donor to P680 and enhance the fluorescence intensity, the electron from hydroxylamine would be transferred to DMBQ and drive the photosynthetic electron flow, rather decreasing the fluorescence intensity. Furthermore, the fluorescence intensity of NBD-PE in the same hybrid membranes did not change upon addition of DMBQ and hydroxylamine, suggesting that the fluorescence changes of

chlorophyll was not caused by direct fluorescence quenching due to the energy transfer to these chemicals (Figure 6E). Although the assay was not directly monitoring the electron transfer, the results supported the premise that reconstituted PSII was capable of transferring electrons. Since the Mn clusters are responsible for the water splitting function in PSII, the effect of hydroxylamine further suggested that the oxygenation function of PSII was retained, although directly detecting generation of oxygen would be necessary in the future studies. The electron transfer from PSII to PQ was further evaluated by using duroquinone that receives electrons from PQ. In the presence of duroquinone, the chlorophyll fluorescence from hybrid thylakoid membranes decreased (Supporting Information, Figure S1). The fluorescence intensity as normalized to the original fluorescence intensity before the addition of duroquinone was 0.279 ± 0.015 (an even greater decrease than with DMBQ). Use of these two different quinones as electron acceptors, and observation of the same effect, further corroborated that the electron transfer activity from PSII to PQ on the substrate was retained.

The activity of reconstituted PSI in the hybrid membranes was assessed by monitoring the generation of NADPH. To provide an excess of electron donors to PSI, reduced DCIP was added to the aqueous solution. At the same time, the activity of PSII was inhibited by adding DCMU during this assay to isolate the activity of PSI from that of PSII. The proteins Fd and FNR, and the reactant $NADP^+$ were added at appropriate concentrations to the aqueous solution and the membrane was illuminated with white light (100 μmol photons m^{-2} s^{-1}). Generation of NADPH by the electron transfer from excited PSI to $NADP^+$ via Fd and FNR was evaluated by taking out the aqueous solution above the hybrid membrane and measuring NADPH fluorescence (excitation at 340 nm and

emission at 450 nm) by the fluorescence spectrometer. The fluorescence from NADPH increased with time (Figure 7A, Supporting Information, Figure S2A). Although we could not estimate the amount of incorporated PSI on the surface, the concentration of NADPH continued to increase with time (Figure 7A), suggesting that the electron transfer was a catalytic reaction. We also ensured that non-ruptured thylakoid membranes were removed from the substrate surface by extensively rinsing with buffer solution (we confirmed the activity of PSI in the suspensions of non-ruptured thylakoid membrane suspensions). In order to confirm that generation of NADPH was due to the light harvesting and electron transfer activities of reconstituted PSI, we conducted the assay using the conditions lacking one of the vital elements, *i.e.* thylakoid membrane, DCIP, Fd and FNR, or light illumination. In either case, NADPH was not generated after incubating 1 h (Figure 7B, Figure S2B). Overall, the results strongly suggested that reconstituted PSI in the hybrid membrane on the substrate retained the electron transfer activity. We assessed the whole electron transfer spanning from PSII through PSI in the hybrid thylakoid membrane by conducting the same assay as Figure 7 without DCMU and reduced DCIP. In this case, however, generation of NADPH upon light illumination was minimal, suggesting that the electron transfer between PSII and PSI was mostly hindered (Supporting Information, Figure S3). Since we confirmed the electron transfer between PSII and PQ, these results may indicate that either cyt b_6/f or plastocyanin (PC) may not properly functioning. One possibility is that PC desorbed from the membrane during the reconstitution process, since it is a water-soluble protein.

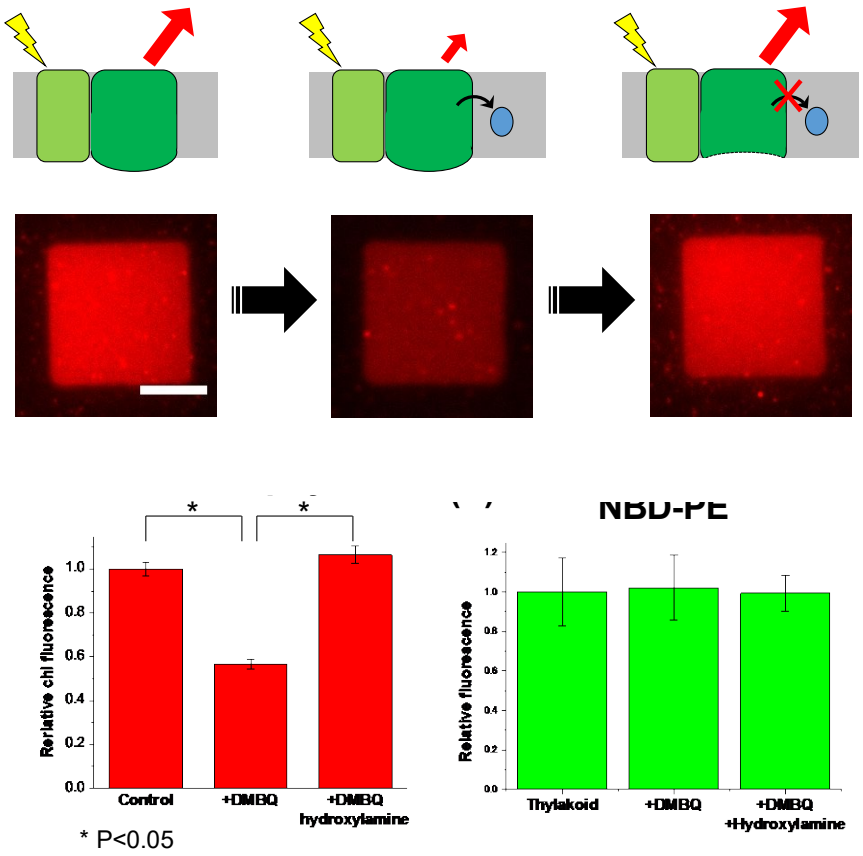

Figure 6. Analysis of the chlorophyll fluorescence from hybrid thylakoid membranes. Fluorescence arises to dissipate the excess energy from excited chlorophyll due to insufficient electron transport (A). The fluorescence intensity decreased upon adding an electron acceptor DMBQ (B), and recovered by further adding hydroxylamine (C). The scale bar corresponds to 10 μm. (D) The relative fluorescence intensities of chlorophyll shown as a bar chart, normalized to the intensity before adding DMBQ. (E) The fluorescence intensities of NBD-PE in the same hybrid membrane were also measured. N= 3 substrates. Error bars represent the standard deviation.

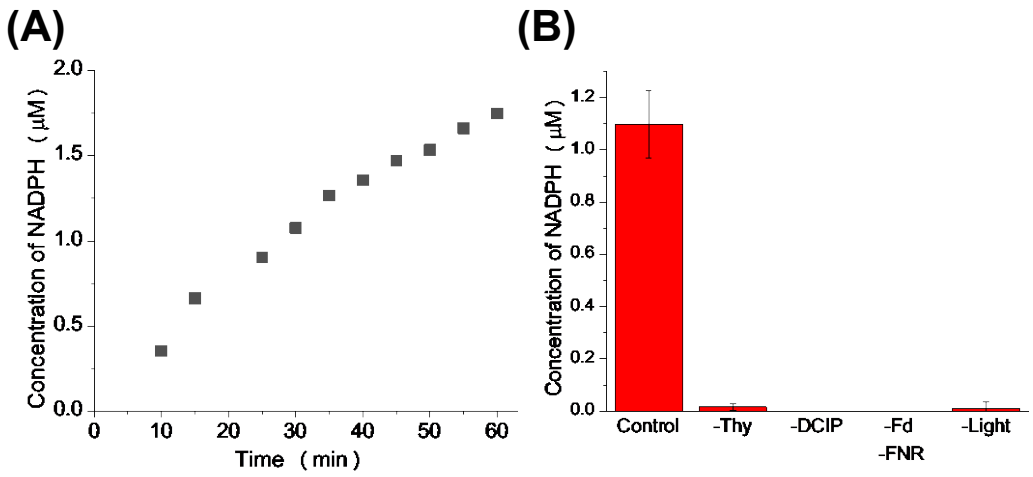

Figure 7. PSI activity of the reconstituted thylakoid was evaluated by measuring the fluorescence of NADPH. (A) Time course of the NADPH fluorescence. (B) Comparison of the NADPH generation with the conditions lacking one of the vital elements, *i.e.* thylakoid membrane (Thy), DCIP, Fd, and FNR, or light illumination. "Control" represents the case with reconstituted thylakoid and all the necessary ingredients. The concentrations of NADPH were calculated from the fluorescence intensity using the calibrated correlation (Supporting Information, Figure S2). N= 3 substrates. Error bars represent the standard deviation.

Conclusions

We developed a methodology to integrate the thylakoid membrane as a continuous 2D membrane in the scaffold of patterned polymeric bilayer. The chlorophyll fluorescence indicated both lateral mobility and electron transfer activity of reconstituted PSII. Furthermore, NADPH could be generated by the electron transfer from photo-excited PSI. The planar, geometrically controlled reconstitution of the excitable thylakoid membranes, instead of purified components, should provide a novel platform to investigate the lateral lipid/ protein organization and interaction of photosynthetic molecules. The polymeric bilayer scaffolds that confine the hybrid thylakoid membrane can potentially enhance the membrane stability by supporting the fluid membrane from the side. Furthermore, the framework would be utilized to transport and concentrate the membrane-bound components by applying electric fields[42,43]. In the present study, we incorporated the whole thylakoid membrane, but it would be interesting to incorporate appressed (grana) and non-appressed (stroma lamellae) thylakoid membranes separately for concentrating some of the membrane components. At the same time, there are some technical limitations at present in the patterned thylakoid membrane. The activity assays in the present study have been rather qualitative due to the lack of information on the amount of reconstituted proteins. In the follow-up study of the 2D thylakoid-lipid hybrid membrane, it is important to quantitate the amount of membrane components in the hybrid membrane on solid substrate. Another important aspect is establishing the whole electron transfer pathway spanning PSII and PSI. In the present study, the electron transfer between PSII and PSI was not efficient, as suggested by the lower efficiency of NADPH generation without a synthetic electron donor to PSI (DCIP). For achieving a "whole thylakoid membrane model" on a chip, we need to address the following technical issues. First, the

molecular orientation needs to be controlled. In the current study, we did not attempt to control the orientation (*i.e.*, the membrane protein "up" or "down" orientation on a solid surface relative to each other). However, by controlling the orientation of purified thylakoid membrane in the vesicular particles, we should be able to have control over the orientation of reconstituted planar thylakoid membrane, since the transformation from vesicular to planar membrane is rather uniform. Second, we would need plastocyanin (PC) proteins to be placed between the substrate and the planar membrane. At present, the distance between the substrate and the membrane is estimated to be ca. 1-2 nm. For incorporating mobile PC proteins, we would need a larger cleft between the substrate and the membrane. One possible approach would be to use a hydrophilic polymer spacer, which can lift the membrane from the substrate surface[44,45]. Complete reconstruction of the whole photosynthetic electron-transfer chain on the substrate would allow quantitative analyses of the complex and sophisticated molecular machines of photosynthesis, which could pave a new avenue for harnessing the solar energy with heightened efficiency. The patterned thylakoid membrane on a chip could also provide a platform to construct an artificial photosynthetic system for generating chemical energy, as exemplified by the ATP synthesis system by exploiting the embedded ATP synthase[46,47].

Supporting Information Available.

The Supporting Information is available free of charge on the ACS Publications website: Effects of duroquinone on the chlorophyll fluorescence, calibration of NADPH concentration from the fluorescence intensity, NADPH generation by the reconstituted

PSII/ PSI electron transfer chain.

Acknowledgements.

This work was supported by Grant-in-Aid for Scientific research (#19H04725) and Japan-UK Research Cooperative Program (JPJSBP120195707) from Japan Society for the Promotion of Science (JSPS). We thank Dr. Toshifumi Takeuchi and Dr. Yukiya Kitayama (Kobe University) for allowing us to use the QCM-D instrument. We thank Dr. Hideto Matsuyama (Kobe University) for allowing us to use the dynamic light scattering instrument. Discussions and helpful comments from Dr. Peter G. Adams, Dr. Stephen D. Evans (University of Leeds), and Dr. Chikahiro Miyake (Kobe University) were appreciated.

References

(1) Allen, J. F.; Forsberg, J. Molecular recognition in thylakoid structure and function. *Trends Plant Sci.* **2001**, *6*, 317-326.

(2) Kirchhoff, H. Architectural switches in plant thylakoid membranes. *Photosynth. Res.* **2013**, *116*, 481-487.

(3) Pribil, M.; Labs, M.; Leister, D. Structure and dynamics of thylakoids in land plants. *J. Exp. Bot.* **2014**, *65*, 1955-1972.

(4) Kramer, D. M.; Sacksteder, C. A.; Cruz, J. A. How acidic is the lumen? *Photosynth. Res.* **1999**, *60*, 151-163.

(5) Ruban, A. V. Quantifying the Efficiency of Photoprotection. *Philos. Trans. R. Soc. Lond. B. Biol. Sci.* **2017**, *372*, 20160393.

(6) Bonardi, V.; Pesaresi, P.; Becker, T.; Schleiff, E.; Wagner, R.; Pfannschmidt, T.; Jahns, P. L., D. Photosystem II core phosphorylation and photosynthetic ccclimation require two different protein kinases. *Nature* **2005**, *437*, 1179-1182.

(7) Iwai, M.; Yokono, M.; Kurokawa, K.; Ichihara, A.; Nakano, A. Live-cell visualization of excitation energy dynamics in chloroplast thylakoid structures. *Sci. Rep.* **2016**, *6*, 29940.

(8) Shimoni, E.; Rav-Hon, O.; Ohad, I.; Brumfeld, V.; Reich, Z. Three-dimensional organization of higher-plant chloroplast thylakoid membranes revealed by electron tomography. *Plant Cell* **2005**, *17*, 2580-2586.

(9) Austin, J. R.; Staehelin, L. A. Three-dimensional architecture of grana and stroma thylakoids of higher plants as determined by electron tomography. *Plant Physiol.* **2011**, *155*, 1601-1611.

(10) Johnson, M. P.; Vasilev, C.; Olsen, J. D.; Hunter, C. N. Nanodomains of cytochrome b6f and photosystem II complexes in spinach grana thylakoid

membranes. *Plant Cell* **2014**, *26*, 3051-3061.

(11) MacGregor-Chatwin, C.; Jackson, P. J.; Sener, M.; Chidgey, J. W.; Hitchcock, A.; Qian, P.; Mayneord, G. E.; Johnson, M. P.; Luthey-Schulten, Z.; Dickman, M. J.; Scanlan, D. J.; Hunter, C. N. Membrane organization of photosystem I complexes in the most abundant phototroph on Earth. *Nat. Plants* **2019**, *5*, 879-889.

(12) Kalyanasundaram, K.; Graetzel, M. Artificial photosynthesis: biomimetic approaches to solar energy conversion and storage. *Curr. Opin. Biotechnol.* **2010**, *21*, 298-310.

(13) Dewa, T.; Sugiura, R.; Suemori, Y.; Sugimoto, M.; Takeuchi, T.; Hiro, A.; Iida, K.; Gardiner, A. T.; Cogdell, R. J.; Nango, M. Lateral organization of a membrane protein in a supported binary lipid domain: Direct observation of the organization of bacterial light-harvesting complex 2 by total internal reflection fluorescence microscopy. *Langmuir* **2006**, *22*, 5412-5418.

(14) Sumino, A.; Dewa, T.; Kondo, M.; Morii, T.; Hashimoto, H.; Gardiner, A. T.; Cogdell, R. J.; Nango, M. Selective assembly of photosynthetic antenna proteins into a domain-structured lipid bilayer for the construction of artificial photosynthetic antenna systems: structural analysis of the assembly using surface plasmon resonance and atomic force microscopy. *Langmuir* **2011**, *27*, 1092-1099.

(15) Adams, P. G.; Vasilev, C.; Hunter, C. N.; Johnson, M. P. Correlated fluorescence quenching and topographic mapping of Light-Harvesting Complex II within surface-assembled aggregates and lipid bilayers. *Biochim. Biophys. Acta* **2018**, *1859*, 1075-1085.

(16) Dewa, T.; Sumino, A.; Watanabe, N.; Noji, T.; Nango, M. Energy transfer and clustering of photosynthetic light-harvesting complexes in reconstituted lipid membranes. *Chem. Phys.* **2013**, *419*, 200-204.

(17) Sumino, A.; Dewa, T.; Noji, T.; Nakano, Y.; Watanabe, N.; Hildner, R.; Bösch, N.; Köhler, J. r.; Nango, M. Influence of Phospholipid Composition on Self-Assembly and Energy-Transfer Efficiency in Networks of Light-Harvesting 2 Complexes. *J. Phys. Chem. B* **2013**, *117*, 10395-10404.

(18) Gräb, O.; Abacilar, M.; Daus, F.; Geyer, A.; Steinem, C. 3D-membrane stacks on supported membranes composed of diatom lipids induced by long-chain polyamines. *Langmuir* **2016**, *32*, 10144-10152.

(19) Seiwert, D.; Witt, H.; Ritz, S.; Janshoff, A.; Paulsen, H. The nonbilayer lipid MGDG and the major light-harvesting complex (LHCII) promote membrane stacking in supported lipid bilayers. *Biochemistry* **2018**, *57*, 2278-2288.

(20) Wang, L.; Roth, J. S.; Han, X.; Evans, S. D. Photosynthetic proteins in supported lipid bilayers: Towards a biokleptic approach for energy capture. *Small* **2015**, *11*, 3306-3318.

(21) Hancock, A. M.; Meredith, S. A.; Connell, S. D.; Jeuken, L. J. C.; Adams, P. G. Proteoliposomes as energy transferring nanomaterials: enhancing the spectral range of light-harvesting proteins using lipid-linked chromophores. *Nanoscale* **2019**, *11*, 16284-16292.

(22) Groves, J. T.; Ulman, N.; Boxer, S. G. Micropatterning fluid lipid bilayers on solid supports. *Science (Washington)* **1997**, *275*, 651-653.

(23) Groves, J. T.; Boxer, S. G. Micropattern formation in supported lipid membranes. *Acc. Chem Res.* **2002**, *35*, 149-157.

(24) Roder, F.; Birkholz, O.; Beutel, O.; Paterok, D.; Piehler, J. Spatial organization of lipid phases in micropatterned polymer-supported membranes. *J. Am. Chem. Soc.* **2013**, *135*, 1189-1192.

(25) Johnson, A.; Bao, P.; Hurley, C. R.; Cartron, M.; Evans, S. D.; Hunter, C. N.; Leggett, G. J. Simple, direct routes to polymer brush traps and nanostructures for studies of diffusional transport in supported lipid bilayers. *Langmuir* **2017**, *33*, 3672-3679.

(26) Morigaki, K.; Baumgart, T.; Offenhäusser, A.; Knoll, W. Patterning solid-supported lipid bilayer membranes by lithographic polymerization of a diacetylene lipid. *Angew. Chem., Int. Ed.* **2001**, *40*, 172-174.

(27) Morigaki, K.; Baumgart, T.; Jonas, U.; Offenhäusser, A.; Knoll, W. Photopolymerization of diacetylene lipid bilayers and its application to the construction of micropatterned biomimetic membranes. *Langmuir* **2002**, *18*, 4082-4089.

(28) Okazaki, T.; Morigaki, K.; Taguchi, T. Phospholipid vesicle fusion on micropatterned polymeric bilayer substrates. *Biophys. J.* **2006**, *91*, 1757-1766.

(29) Takagi, D.; Ifuku, K.; Nishimura, T.; Miyake, C. Antimycin A inhibits cytochrome b559-mediated cyclic electron flow within photosystem II. *Photosynth. Res.* **2019**, *139*, 487-498.

(30) Arnon, D. I. Copper enzymes in isolated chloroplasts. Polyphenoloxidase in beta vulgaris. *Plant Physiol.* **1949**, *24*, 1-15.

(31) Morigaki, K.; Kimura, S.; Okada, K.; Kawasaki, T.; Kawasaki, K. Formation of substrate supported membranes from mixtures of long and short chain phospholipids. *Langmuir* **2012**, *28*, 9649-9655.

(32) Morigaki, K.; Schönherr, H.; Okazaki, T. Polymerization of diacetylene phospholipid bilayers on solid substrate: Influence of the film deposition temperature *Langmuir* **2007**, *23*, 12254-12260.

(33) Murphy, D. J.; Woodrow, I. E. Lateral heterogeneity in the distribution of thylakoid membrane lipid and protein components and its implications for the molecular organisation of photosynthetic membranes. *Biochim. Biophys. Acta* **1983**, *725*, 104-112.

(34) Okazaki, T.; Inaba, T.; Tatsu, Y.; Tero, R.; Urisu, T.; Morigaki, K. Polymerized lipid bilayers on solid substrate: Morphologies and obstruction of lateral diffusion. *Langmuir* **2009**, *25*, 345-351.

(35) Dodd, C. E.; Johnson, B. R. G.; Jeuken, L. J. C.; Bugg, T. D. H.; Bushby, R. J.; Evans, S. D. Native *E. coli* inner membrane incorporation in solid-supported lipid bilayer membranes. *Biointerphases* **2008**, *3*, FA59-FA67.

(36) Richards, M. J.; Hsia, C.-Y.; Singh, R. R.; Haider, H.; Kumpf, J.; Kawate, T.; Daniel, S. Membrane protein mobility and orientation preserved in supported bilayers created directly from cell plasma membrane blebs. *Langmuir* **2016**, *32*, 2963-2974.

(37) Reimhult, E.; Höök, F.; Kasemo, B. Vesicle adsorption on SiO_2 and TiO_2: dependence on vesicle size. *J. Chem. Phys.* **2002**, *117*, 7401-7404.

(38) Haferkamp, S.; Kirchhoff, H. Significance of molecular crowding in grana membranes of higher plants for light harvesting by photosystem II. *Photosynth. Res.* **2008**, *95*, 129-134.

(39) Kirchhoff, H.; Haferkamp, S.; Allen, J. F.; Epstein, D. B. A.; Mullineaux, C. W. Protein diffusion and macromolecular crowding in thylakoid membranes. *Plant Physiol.* **2008**, *146*, 1571-1578.

(40) Keller, C. A.; Kasemo, B. Surface specific kinetics of lipid vesicle adsorption measured with a quartz crystal microbalance. *Biophys. J.* **1998**, *75*, 1397-1402.

(41) Krieger, A.; Weis, E. The role of calcium in the pH-dependent control of Photosystem II. *Photosynth. Res.* **1993**, *37*, 117-130.

(42) van Oudenaarden, A.; Boxer, S. G. Brownian ratchets: Molecular separations in lipid bilayers supported on patterned arrays. *Science (Washington)* **1999**, *285*, 1046-1048.

(43) Cheetham, M. R.; Bramble, J. P.; McMillan, D. G. G.; Bushby, R. J.; Olmsted, P. D.; Jeuken, L. J. C.; Evans, S. D. Manipulation and sorting of membrane proteins using patterned diffusion diffusion-aided ratchets with AC fields in supported lipid bilayers. *Soft Matter* **2012**, *8*, 5459-5465.

(44) Tanaka, M.; Sackmann, E. Polymer-supported membranes as models of the cell surface. *Nature* **2005**, *437*, 656-663.

(45) Nishimura, T.; Tamura, F.; Kobayashi, S.; Tanimoto, Y.; Hayashi, F.; Sudo, Y.;

Iwasaki, Y.; Morigaki, K. Hybrid model membrane combining micropatterned lipid bilayer and hydrophilic polymer brush. *Langmuir* **2017**, *33*, 5752-5759.

(46) Li, Y.; Fei, J.; Li, G.; Xie, H.; Yang, Y.; Li, J.; Xu, Y.; Sun, B.; Xia, J.; Fu, X.; Li, J. Supramolecular assembly of photosystem II and adenosine triphosphate synthase in artificially designed honeycomb multilayers for photophosphorylation. *ACS Nano* **2018**, *12*, 1455-1461.

(47) Li, G.; Fei, J.; Xu, Y.; Li, Y.; Li, J. Bioinspired assembly of hierarchical light-harvesting architectures for improved photophosphorylation. *Adv. Funct. Mater.* **2018**, *28*, 1706557.

TOC:

Reconstituted thylakoid membrane